Observational Study

Medicine®

OPEN

Diagnostic value of a spiral breast computed tomography system equipped with photon counting detector technology in patients with implants

An observational study of our initial experiences

Lisa Ruby, MD*, Sojin Shim, MSc, Nicole Berger, MD, Magda Marcon, MD, Thomas Frauenfelder, MD, Andreas Boss, MD, PhD

Abstract

To evaluate the value of a breast computed tomography (CT) (B-CT) in assessing breast density, pathologies and implant integrity in women with breast implants.

This retrospective study was approved by the local ethics committee. B-CT images of 21 women with implants (silicone/saline; 20 bilateral, 1 unilateral) who underwent opportunistic screening or diagnostic bilateral B-CT were included. Breast density, implant integrity, extensive capsular fibrosis, soft tissue lesions and micro-/macrocalcifications were rated. In 18 of the 21 women, an additional ultrasound and in two patients breast magnetic resonance imaging was available for comparison. The average dose was calculated for each breast using verified Monte Carlo simulations on 3D image data sets.

Breast density was nearly completely fatty (ACR a) in two patients, scattered fibroglandular (ACR b) in five, heterogeneously dense (ACR c) in ten and very dense (ACR d) in four women. In three women showed a unilateral positive Linguine sign indicative of an inner capsule rupture. Extensive capsular fibrosis was found in three women. In three women, soft tissue lesions were depicted, which revealed to be cysts (n = 2) and lymph nodes (n = 1) on subsequent sonography. Diffuse, non-clustered microcalcifications were found in nine women. Eleven women showed cutaneous or intramammary macrocalcifications. Average dose was 6.45 mGy (range 5.81–7.28 mGy).

In women with implants, B-CT presents a promising modality for evaluating breast density, implant integrity, extensive capsular fibrosis, soft tissue lesions and micro-/macrocalcifications without the need of breast compression utilizing a lower dose compared to doses reported for conventional four-view mammography.

Abbreviations: ABUS = automated breast ultrasound, B-CT = breast computed tomography, CT = computed tomography, MC = Monte Carlo, MRI = magnetic resonance imaging.

Keywords: breast, breast implants, breast neoplasms, spiral computed tomography

Editor: Oguzhan Ekizoglu.

The authors have no funding and no conflicts of interest to disclose.

The datasets generated during and/or analyzed during the current study are not publicly available, but are available from the corresponding author on reasonable request.

Institute of Diagnostic and Interventional Radiology, University Hospital Zurich, Rämistrasse, Zürich, Switzerland.

** Correspondence: Lisa Ruby, Institute of Diagnostic and Interventional Radiology, University Hospital Zurich, Rämistrasse 100, 8091 Zürich, Switzerland (e-mail: lisa.ruby@usz.ch).*

How to cite this article: Ruby L, Shim S, Berger N, Marcon M, Frauenfelder T, Boss A. Diagnostic value of a spiral breast computed tomography system equipped with photon counting detector technology in patients with implants: An observational study of our initial experiences. Medicine 2020;99:30(e20797).

Received: 11 January 2020 / Received in final form: 30 April 2020 / Accepted: 21 May 2020

http://dx.doi.org/10.1097/MD.0000000000020797

1. Introduction

In 2018, 313.735 women and teenagers underwent breast augmentation surgery using silicone (88%) or saline (12%) implants and 29.236 women had breast implants removed in the United States.[1] Implants come along with a number of problems, such as implant rupture,[2] capsular contracture as well as difficult breast cancer screening and diagnosis,[3,4] which can be challenging for radiologists.

Four-view mammography presents the current reference standard for breast cancer screening in women with implants according to the guidelines of the American Cancer Society (ACS).[5,6] Augmentation mammography comes with the disadvantage of a higher mean glandular dose due to decreased compression as well as radiation absorption of the implant itself.[7,8] The discomfort caused by compression during mammography can be particularly enhanced in women with implants. Mammography cannot, in most of the cases, detect intracapsular ruptures, which account for the majority of mplant failures.[9] In addition, although very rare, mechanical pressure during mammography can lead to implant rupture.[10]

Ultrasound presents a moderately good modality in augmented breasts as implant integrity can be assessed,[11] but it is not sufficient for breast cancer screening as a stand-alone method.[12]

Magnetic resonance imaging (MRI) is the most accurate modality for the evaluation of implant integrity in women with implants.[13–16] The United States Food and Drug Administration recommends a primary MRI screening three years after implant insertion and every two years afterwards to detect silicone rupture.[17] However, the high costs, multiple contraindications (metals, claustrophobia) as well as the inability to detect or characterize calcifications that come with MRI have led to a demand for an additional modality in women with implants. Currently, there are not specific recommendations to use breast MRI for breast cancer screening purpose in women with implants.

Therefore, there is a demand for a modality, which can combine the advantages of both mammography and MRI in terms of calcification detection and implant integrity assessment. Spiral breast computed tomography (CT) (B-CT) with a photon-counting detector offers a fast examination, providing high-quality images without the need of compression or contrast agent application.[18] Berger and Marcon et al. have demonstrated the capability of the B-CT to detect soft tissue lesions as well as micro- and macrocalcifications, serving as an alternative method for conventional mammography, especially in those patients not willing to undergo a mammography exam because of breast compression.[18,19] However, the value of this new technology in assessing implant integrity, breast density and pathologies has not been evaluated for patients with implants in the literature.

The purpose of this study was to investigate the potential of a spiral B-CT in evaluating breast density, implant integrity, extensive capsular fibrosis, soft tissue lesions as well as micro- and macrocalcifications in breasts augmented by implants.

2. Methods

All breast CTs performed at our institute in the timeframe 01/2018–09/2019 were analyzed retrospectively. The study was approved by the local ethics committee (Kantonale Ethikkommission Zürich; approval number: 2016–00064). Written informed consent was obtained from all women. B-CT examinations were performed in women with breast implants undergoing opportunistic breast cancer screening, in patients with a history of breast cancer or in symptomatic patients (mastodynia, palpation findings). Breast CT was offered as an alternative modality for patients refusing the indicated mammography or MRI exam due to inherent breast compression or contrast agent application. For all symptomatic patients, women with a finding or dense breast tissue on breast CT, a supplemental ultrasound examination of both breasts was performed either using a handheld ultrasound system (Philips iU22A, Philips or Logiq E9, GE Healthcare) or automated breast ultrasound (Invenia ABUS, GE Healthcare).

2.1. Breast-CT (B-CT)

All women were placed in prone position in a spiral breast CT (nu:view; AB-CT [Advanced Breast CT] GmbH). Each breast was examined separately starting with the left side. The detector is equipped with telluride crystals and the detector area has a total size of 280×500 mm. A fixed x-ray tube voltage of 60 kV and a tube current of 32 mAs were used for all patients (at the beginning breast CT examinations at our institution were performed with 25 mAs, later changing the settings to 32 mAs for better depiction of microcalcifications). All examinations were performed with the nu:view reconstruction software, which utilizes a Feldkamp-type filtered back-projection algorithm for image reconstructions. A voxel size of $300\,\mu m^3$ and 4×4 detector binning were used for the standard image reconstruction, whereas a kernel of $150\,\mu m^3$ voxel size with 2×2 detector binning was used for a high-resolution image reconstruction. Images were reconstructed to a size of 0.3 mm for the standard and 0.15 mm for the high-resolution images. The images were analyzed on a picture archiving and communication system workstation equipped with a customized breast imaging display software (AGFA Impax 6), enabling sagittal and coronal reformations as well as maximum intensity projections (MIP).

2.2. Reading and statistical evaluation

Using the report by the reporting radiology resident confirmed by an experienced radiologist (experience >15 years), the images were additionally descriptively analyzed by a second-year radiology resident. Breast density was visually assessed for each patient; lobular involution was defined as <25% parenchyma, fibroglandular-scattered as 25% to 50% parenchyma, heterogeneously dense as 51% to 75% parenchyma, extremely dense as >75% parenchyma.[20] Images were analyzed regarding the presence of the following features: implant location (epipectoral/subpectoral), intra-/extracapsular implant rupture, extensive capsular fibrosis (defined as soft-tissue-isodense material with calcifications surrounding the implant), soft tissue lesions and micro-/macrocalcifications.

2.3. Dose calculation

Radiation dose was calculated by Monte Carlo (MC) simulations using a commercially available validated tool.[21–23] 1.0E6 photon histories were simulated for each MC calculation. The results of the MC simulations were normalized by the air kerma of 18.12 mGy per 100 mAs. The average dose of each breast was calculated in the segmented glandular tissue regions based on Hounsfield Unit thresholding.

3. Results

3.1. Patient characteristics

21 women (median age 50.5 years, range 35–72 years) with breast implants (silicone or saline; 20 bilateral, 1 unilateral) who underwent bilateral B-CT were included in the study. The woman with a unilateral implant had a history of multi-centric, invasive ductal breast cancer in the right breast, which was treated with segmentectomy and radiation therapy. Apart from this patient, none of the included women had a history of breast cancer. 5/21 (23.8%) had a first or second degree relative with breast cancer, 16/21 did not have a first or second degree relative with breast cancer. For 18/21 women (85.7%), an additional ultrasound examination was performed on the day of the B-CT examination (15 handheld ultrasound, 3 ABUS). For two women (9.5%), previous MRI exams were available.

3.2. Breast density

2/21 (10%) breasts showed (complete) lobular involution (Fig. 1A), 5/21 (24%) were fibroglandular scattered (Fig. 1B), 10/21 (48%)

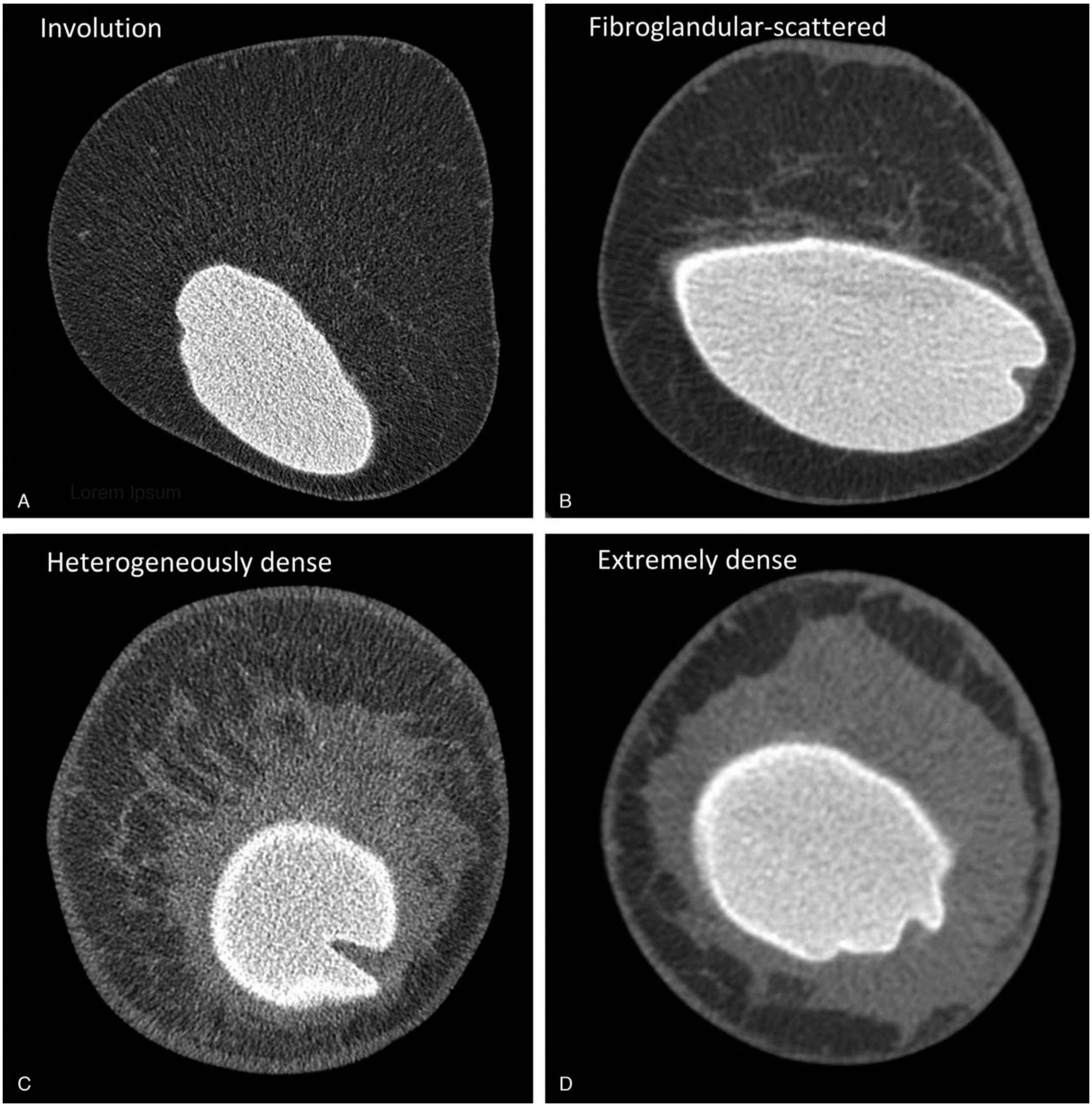

Figure 1. A-D. Coronal view of B-CT images. The figure displays the implant embedded in breasts of different density, showing A) lobular involution, B) fibroglandular-scattered, C) heterogeneously dense and D) extremely dense tissue.

were heterogeneously dense (Fig. 1C), whereas 4/21 (19%) were extremely dense (Fig. 1D). In the fibroglandular dense type, glandular tissue adapted to the form of the implant showing a parallel alignment to the implant borders (arrows in Fig. 1B), whereas for the other three density types no such pattern was found.

3.3. Breast implants

For 7/21 patients, implants were located subpectorally, whereas for 14/21 patients, implants were located epipectorally. Silicone exhibited a notably higher density corresponding to higher X-ray attenuation compared to glandular tissue and fat. Intermediate density was observed for the plastic material of the implant coating. Nearly identical density was found for glandular tissue and the pectoral muscle.

In 3/21 (14%) women, a unilateral implant rupture was detected. Fig. 2 demonstrates breast CT images and corresponding automated breast ultrasound (ABUS) images of a 35-year old woman with a first degree family history of breast cancer and bilateral implants for six years, who rejected an MRI exam due to the associated contrast agent application. Both modalities revealed implant folds in the left breast (Figs. 2A and C) and a positive Linguine sign in the right breast (Figs. 2B and D), indicative of an intracapsular rupture.

Extensive capsular fibrosis was detected in 3/21 (14%) women. Fig. 3 displays severe calcifications in a 62-year old woman with a

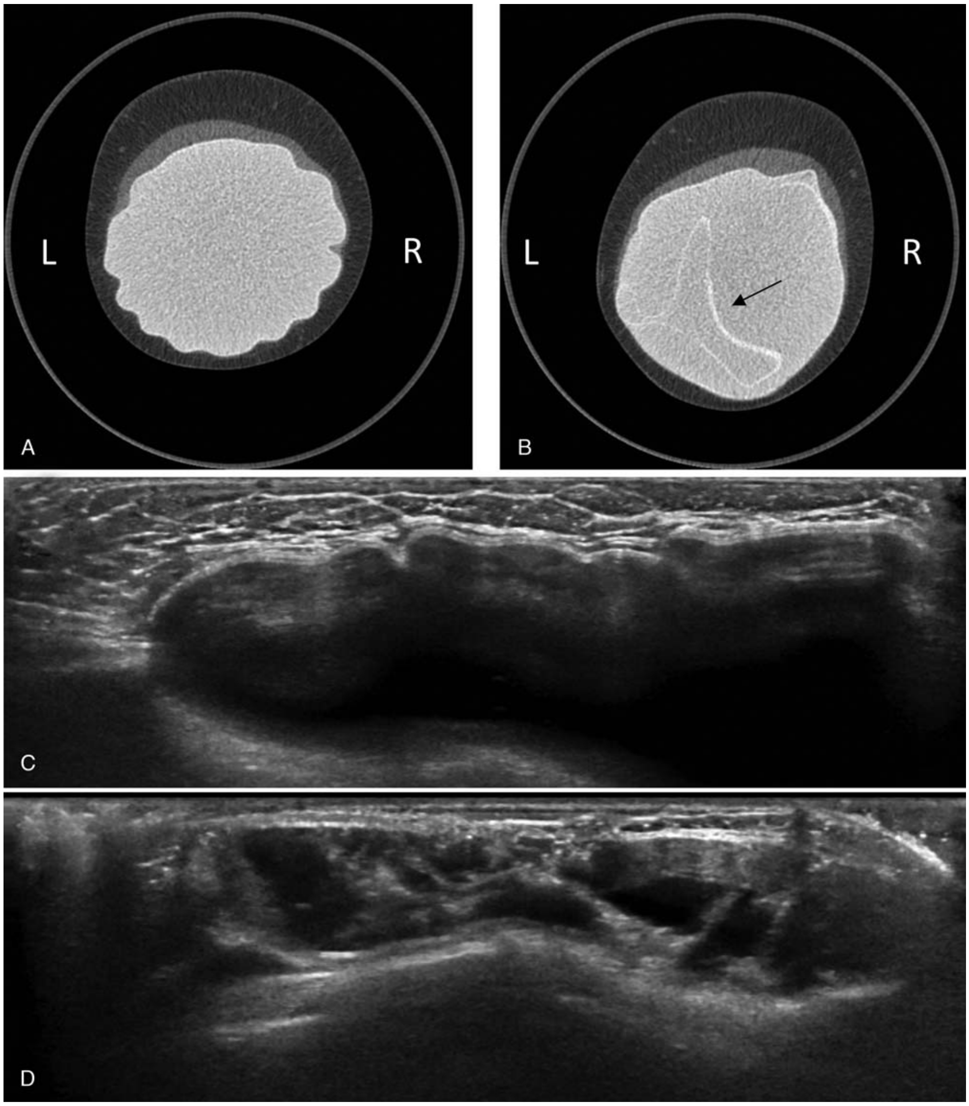

Figure 2. A-D. A 35-year old woman presenting with a family history of breast cancer (mother who was diagnosed with breast cancer at the age of 40 yrs) and bilateral gel implants for six yrs. Breast CT revealed implant folds in the left breast (A) and a positive Linguine sign in the right breast (B), indicative of an intracapsular rupture (coronal views, respectively). Automated breast ultrasound (ABUS) confirmed the observed findings for the left (C) and right (D) breasts.

history of bilateral implants for 46 years, who presented to our clinic with severe discomfort due to bilateral breast induration.

3.4. Breast lesions

Intramammary soft tissue lesions were found in 3/21 (14%) women, two revealed to be simple cysts and the third an intramammary lymph node. Fig. 4 shows an intramammary lesion in a 48-year old, asymptomatic woman with a six-year history of bilateral implants who presented for routine breast cancer screening. B-CT displayed a 10 x 6 mm measuring, oval soft tissue mass at 1–2 o'clock (Fig. 4A). A subsequent ultrasound examination (Fig. 4B) depicted a sharply aligned, anechoic lesion with dorsal acoustic enhancement, which was interpreted as a simple cyst.

Microcalcifications were found in 9/21 (43%), macrocalcifications or cutaneous calcifications in 11/21 (52%) of the included patients. No clustered or otherwise suspicious microcalcifications were found. Exemplary typical intramammary micro- (Fig. 5A and C) and macrocalcifications (Figs. 5B and D) after several implant revision surgeries are shown in a 65-year old woman.

3.5. Intermodality comparison B-CT vs. MRI

Previously acquired MRI images were available for 2/21 (10%) women. To illustrate the comparison between B-CT and MRI (MRI images were acquired 2 years prior to the B-CT examination), the images of a 35-year old woman with a family history of breast cancer who presented to our clinic for a screening examination are shown in Fig. 6. From the example images, it can be seen that the B-CT images exhibit features of both, T1-weighted and silicone–selective T2-weighted images with clear depiction of breast parenchyma and high density of the implants. In the MRI silicone-selective sequence, no parenchymal

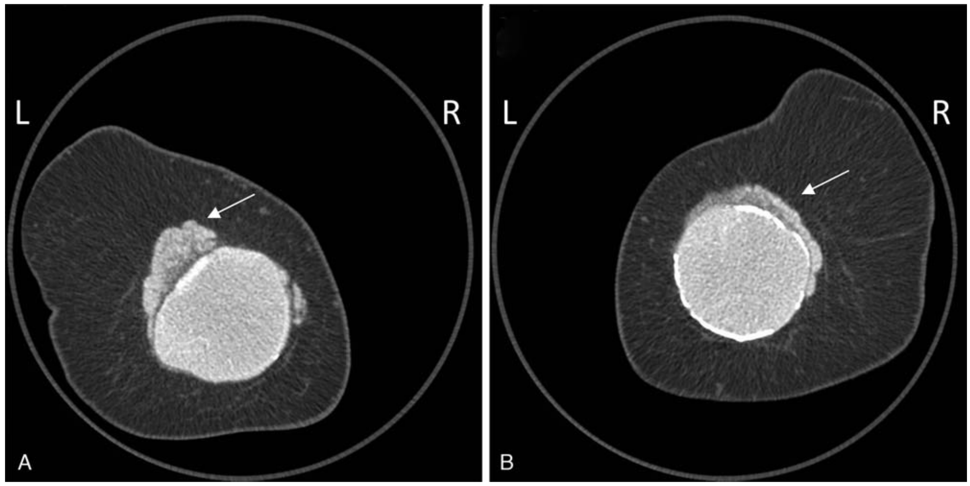

Figure 3. A, B. A 62-yr old woman with bilateral breast implants for 46 yrs. She presented to our clinic with bilateral breast induration. Severe calcifications surrounding the implant can be seen bilaterally in the coronal breast CT images on the left A) and right B) side.

tissue is depicted, whereas in the T1-weighted image, the silicone implant shows low signal intensity.

3.6. Average dose

Including all B-CT measurements for the 21 women, we found an average dose of 6.45 mGy (SD 0.36; range 5.81–7.28 mGy) (Table 1). For the patient with a unilateral implant (patient 15), we calculated a dose of 6.21 mGy (SD 0.12 mGy) for the right (implant) breast and 6.15 mGy (SD 0.12 mGy) for the left (non-implant) breast.

4. Discussion

Our results demonstrate the potential clinical value of a spiral B-CT in evaluating breast density, implant integrity, extensive capsular fibrosis, intramammary soft tissue lesions as well as micro- and macrocalcifications in women with breast implants without the need of contrast agent application or painful breast compression. It is the only modality providing both, excellent depiction of implants and microcalcifications in a single examination without overlay effects.

MRI of the breast presents the most accurate method to assess implant integrity.[13–16] However, the high costs and multiple contraindications (metals, claustrophobia) that come with MRI have led to a demand for an additional modality in women with implants. Furthermore, assessment of microcalcifications is hardly possible in MRI,[24–26] which is particularly important for the diagnosis of breast cancer precursors and lesions of unknown malignant potential (B3 lesions).

Mammography, which presents the screening method of choice for women with implants in some countries,[5,6] comes with the disadvantage of a higher mean glandular dose in augmented breasts due to decreased compression as well as radiation absorption of the implant itself.[7,8] Recommended four-view augmentation mammography is associated with a more than threefold mean glandular dose (10.7 mGy) compared to conventional two-view mammography (3.4 mGy).[8] For the

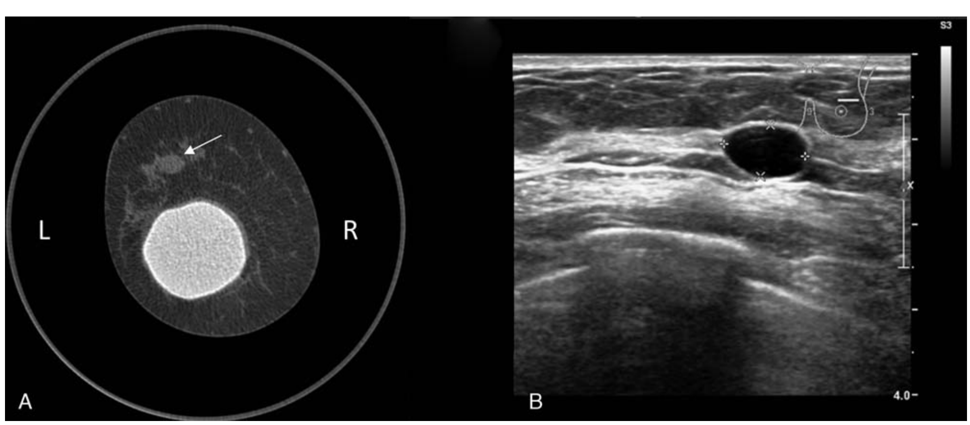

Figure 4. A, B. A 48-yr old, asymptomatic woman with a history of bilateral gel implants for six yrs presented for routine breast cancer screening. The displayed coronal B-CT image (A) shows a 10 x 6 mm measuring, oval consolidation at 1-2 o'clock. A subsequent sonographic exam (B) showed a sharply aligned, anechoic lesion with dorsal acoustic enhancement, which was interpreted as a simple cyst.

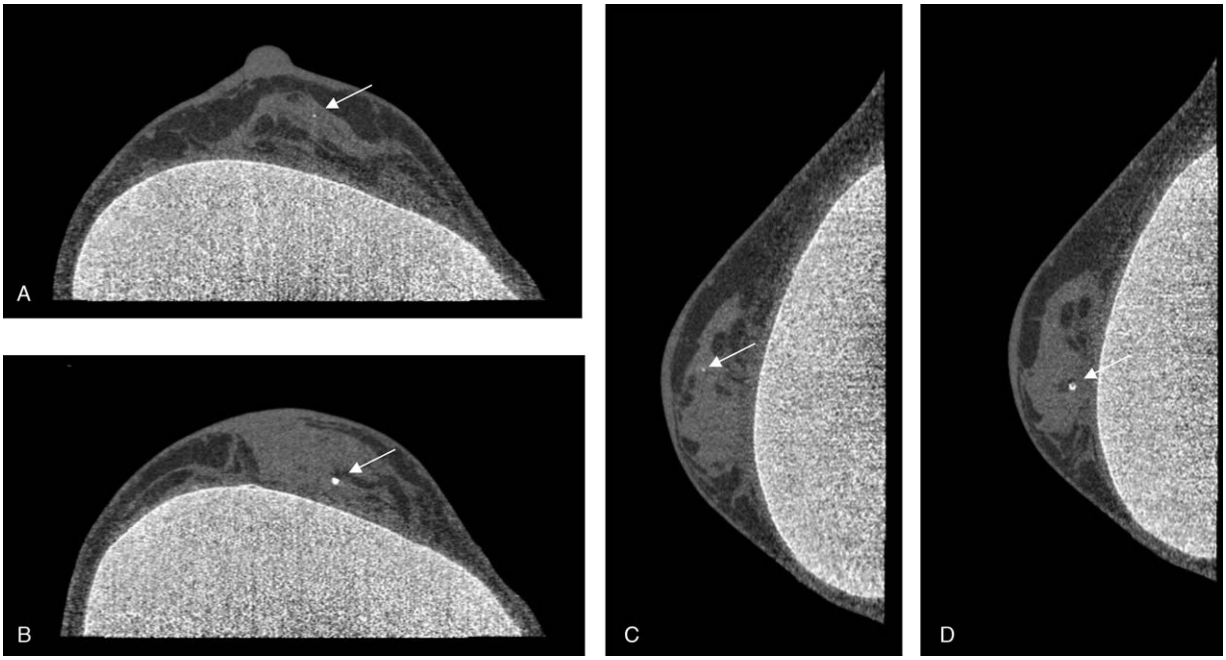

Figure 5. A-D. Single micro- (A,C) and macrocalcifications (B, D) are displayed in the axial (A,B) and sagittal (C,D) plane in a 65-yr old woman with bilateral gel implants, which required several revision surgeries.

breast CT, we found an average dose of 6.45 mGy (SD 0,36; range 5.81 7.28 mGy) in women with implants. In comparison, Berger and Marcon et al. calculated a dose of 5.08 mGy (range 4.4–5.7 mGy) in a screening population without implants using the same spiral breast CT system.[19] Although, to the best of our knowledge, no recent clinical studies have proven an inferior diagnostic performance of mammography in women with implants compared to women without implants, in a MC simulation study it has been shown that silicone gel implants thicker than 26 mm for the case of mammography and 14 mm for the case of B-CT obscured the visibility of underlying structures, such as soft tissue masses and microcalcifications.[27] In B-CT, due to the possibility to obtain cross-sectional images rather than projection images as in mammography, not only the superimposition of the implant but also of the glandular tissue can be reduced.

According to Berger and Marcon et al., B-CT provides similar information with regard to soft tissue lesion detection without superimposition compared to mammography.[18,19] In line with this, we were able to detect intramammary soft tissue lesions in patients with implants. Features, such as density (Hounsfield units), shape and margins, help in the differentiation of the lesions. However, similar to mammography, the potential in differentiating structures of similar density, such as very dense breast tissue and soft tissue lesions, but also mild fibrosis and mild peri-implant fluid, is limited. Therefore, ultrasound remains an indispensable, complementary method for the further classification of lesions detected on mammography or CT, in symptomatic women, women with dense breasts and for the assessment of implant integrity.[11,28,29] Although ultrasound has undergone remarkable improvement in recent years with increased resolution and the utilization of additional parameters, such as elastic modules, it is by itself not sufficient for breast cancer screening and diagnosis as a stand-alone method due to its decreased sensitivity in detecting DCIS and small tumors in breasts characterized by shadowing and fibrocystic changes.[29–31] B-CT covers these limitations. Moreover, ultrasound is a very examiner-dependent modality,[29] whereas for the B-CT, images are acquired in a reproducible way and can be analyzed by a second radiologist at a later time point. Regarding the radiation exposure that comes with the B-CT in contrast to ultrasound, the benefits of mammographic screening with a remarkable mortality reduction have been shown to outweigh the comparably small risk of radiation-induced cancer and should therefore not prevent women above the age of 40 from undergoing screening mammography or the alternative B-CT,[32–34] which is associated with a comparable dose compared to mammography.[18,19,35] We want to point out that we do not regard breast-CT and ultrasound as competing modalities but rather as modalities complementing each other.

Considering the costs of both, B-CT and ultrasound, as with any novel technique with only a few devices available worldwide, purchase costs of the B-CT are high compared to ultrasound devices. However, a decrease in costs over time can be expected with a widespread use of this method and competing vendors. At our institute, B-CT examination costs are equivalent to that of mammography (CHF 193) and slightly higher compared to ultrasound (CHF 165).

Examination and interpretation times of mammography and B-CT are very short (5 minutes) for both breasts, whereas examination times of a thorough ultrasound exam performed by a radiologist range between 25 and 30 minutes,[36] which also results in higher costs.

The potential of dual-energy CT in the assessment of implant integrity has been shown in the literature.[37,38] The linguine sign,[13] which represents the collapsed implant shell in the gel showing a high sensitivity and specificity for an intracapsular rupture,[39] was identified with the B-CT, in spite of the single energy spectrum applied.

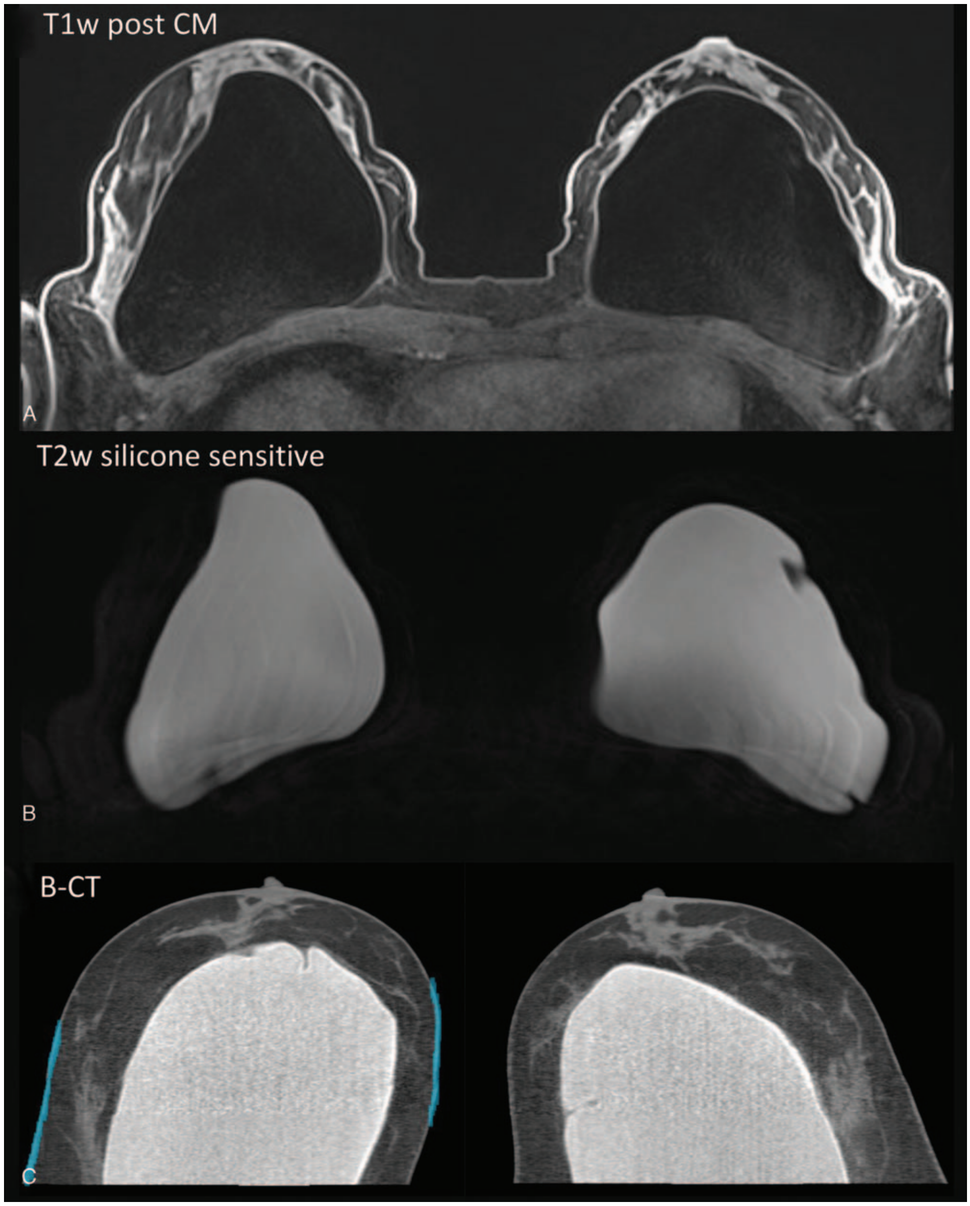

Figure 6. A-C. Magnetic resonance images (T1w with contrast (A) and silicone-seletive T2w (B)) acquired two yrs prior and B-CT images (C) of a 35-yr old woman with a family history of breast cancer and a history of epipectoral gel implants for more than ten yrs, who presented for a screening examination, are shown. Both implants are intact with small folds. The B-CT images exhibit features of both, T1w and silicone–selective T2w images with clear depiction of breast parenchyma and high density of the silicone implants. In the MRI silicone-selective sequence, no parenchymal tissue is depicted, whereas in the T1w image, the silicone implant shows low signal intensity. CT = computed tomography, MRI = magnetic resonance imaging.

Limitations of our study include the missing direct comparison with MRI or mammography regarding the detection of pathologies and comparison of dose (B-CT vs. mammography). Further limitations are the low number of women with implants in the given study period, the lack of patients with breast cancer diagnosis and implants, the missing follow-up examinations as well as the retrospective study design. However, our initial experiences demonstrate a great potential of this novel B-CT technique in evaluating augmented breasts, which might become the modality of choice for fast and time-efficient breast imaging in patients with implants.

Giving an outlook, further steps, which aim at improving the differentiation of lesions, might include the application of iodine contrast agents.[40] Moreover, as a further technical milestone, phase contrast B-CT might strongly improve the specificity of microcalcification assessment.[41,42]

In conclusion, B-CT presents a promising modality for implant integrity assessment and breast cancer screening in women with implants without a need of breast compression, utilizing a lower dose compared to reported doses for conventional four-view mammography.

Acknowledgments

We thank Christian Steiding PhD and Daniel Kolditz PhD, AB-CT Advanced Breast-CT GmbH, for their technical support throughout the study.

Table 1

Average dose.

Patient Number	Breast	Average dose [mGy]	SD Average dose [mGy]
1	L	6.19	0.1238
	R	6.21	0.1242
2	L	6.31	0.1262
	R	6.21	0.1242
3	L	6.53	0.1306
	R	6.66	0.1332
4	L	6.42	0.1284
	R	6.45	0.129
5	L	6.12	0.1224
	R	5.91	0.1182
6	L	6.02	0.1204
	R	5.93	0.1186
7	L	6.87	0.1374
	R	6.66	0.1332
8	L	6.74	0.1348
	R	6.59	0.1318
9	L	6.31	0.1262
	R	6.28	0.1256
10	L	7.28	0.1456
	R	7.01	0.1402
11	L	5.81	0.1162
	R	6.14	0.1228
12	L	6.34	0.1268
	R	6.5	0.13
13	L	6.08	0.1216
	R	5.94	0.1188
14	L	6.39	0.1278
	R	6.32	0.1264
15	L	6.15	0.123
	R	6.21	0.1242
16	L	6.99	0.1398
	R	6.93	0.1386
17	L	6.83	0.1366
	R	6.74	0.1348
18	L	6.44	0.1288
	R	6.48	0.1296
19	L	7.03	0.1406
	R	7.06	0.1412
20	L	6.16	0.1232
	R	6.11	0.1222
21	L	6.95	0.139
	R	6.67	0.1334

Average dose and standard deviation (SD) are displayed for each breast (L, left; R, right) of the 21 women. All patients had bilateral implants, except for patient 15, who had a unilateral implant on the right side.

Author contributions

Conceptualization: Lisa Ruby, Andreas Boss.
Data curation: Lisa Ruby, Sojin Shim.
Formal analysis: Lisa Ruby, Andreas Boss.
Investigation: Lisa Ruby, Andreas Boss.
Methodology: Lisa Ruby, Andreas Boss.
Project administration: Lisa Ruby, Nicole Berger, Magda Marcon, Thomas Frauenfelder, Andreas Boss.
Resources: Lisa Ruby, Sojin Shim, Nicole Berger, Magda Marcon, Thomas Frauenfelder, Andreas Boss.
Software: Sojin Shim, Andreas Boss.
Supervision: Lisa Ruby, Andreas Boss.
Validation: Lisa Ruby.
Visualization: Lisa Ruby.
Writing – original draft: Lisa Ruby, Andreas Boss.
Writing – review & editing: Lisa Ruby, Sojin Shim, Nicole Berger, Magda Marcon, Thomas Frauenfelder, Andreas Boss.

References

[1] Surgeons ASoP. 2018 National Plastic Surgery Statistics. 2018.
[2] Seigle-Murandi F, Lefebvre F, Bruant-Rodier C, et al. Incidence of breast implant rupture in a 12-year retrospective cohort: evidence of quality discrepancy depending on the range. J Plast Reconstr Aesthet Surg 2017;70:42–6.
[3] Araco A, Caruso R, Araco F, et al. Capsular contractures: a systematic review. Plast Reconstr Surg 2009;124:1808–19.
[4] Uematsu T. Screening and diagnosis of breast cancer in augmented women. Breast Cancer 2008;15:159–64.
[5] Oeffinger KC, Fontham ET, Etzioni R, et al. Breast cancer screening for women at average risk: 2015 guideline update from the American Cancer Society. JAMA 2015;314:1599–614.
[6] ACS. American Cancer Society Breast Cancer Screening Guideline. Available at: https://www.cancer.org/health-care-professionals/american-cancer-society-prevention-early-detection-guidelines/breast-cancer-screening-guidelines.html. Published 2019. Accessed 04/09/2020.
[7] Couto LS, Freitas-Junior R, Correa RS, et al. Mean glandular dose in digital mamography in women with breast implants. J Radiol Prot 2019;39:498–510.
[8] Smathers RL, Boone JM, Lee LJ, et al. Radiation dose reduction for augmentation mammography. AJR Am J Roentgenol 2007;188: 1414–21.
[9] Seiler SJ, Sharma PB, Hayes JC, et al. Multimodality imaging-based evaluation of single-lumen silicone breast implants for rupture. Radiographics 2017;37:366–82.
[10] Feng LJ, Amini SB. Analysis of risk factors associated with rupture of silicone gel breast implants. Plast Reconstr Surg 1999;104:955–63.
[11] Telegrafo M, Moschetta M. Role of US in evaluating breast implant integrity. J Ultrasound 2015;18:329–33.
[12] Evans A, Trimboli RM, Athanasiou A, et al. Breast ultrasound: recommendations for information to women and referring physicians by the European Society of Breast Imaging. Insights Imaging 2018; 9:449–61.
[13] Juanpere S, Perez E, Huc O, et al. Imaging of breast implants-a pictorial review. Insights Imaging 2011;2:653–70.
[14] Di Benedetto G, Cecchini S, Grassetti L, et al. Comparative study of breast implant rupture using mammography, sonography, and magnetic resonance imaging: correlation with surgical findings. Breast J 2008; 14:532–7.
[15] Hold PM, Alam S, Pilbrow WJ, et al. How should we investigate breast implant rupture? Breast J 2012;18:253–6.
[16] Mann RM, Balleyguier C, Baltzer PA, et al. Breast MRI: EUSOBI recommendations for women's information. Eur Radiol 2015;25: 3669–78.
[17] FDA. FDA update on the safety of silicone gel-filled breast implants. FDA. Published 2011. Accessed May 26, 2019. https://www.fda.gov/medical-devices/breast-implants/update-safety-silicone-gel-filled-breast-implants-2011-executive-summary.
[18] Berger N, Marcon M, Frauenfelder T, et al. Dedicated spiral breast computed tomography with a single photon-counting detector: initial results of the first 300 women. Invest Radiol 2020;55:68–72.
[19] Berger N, Marcon M, Saltybaeva N, et al. Dedicated breast computed tomography with a photon-counting detector: initial results of clinical in vivo imaging. Invest Radiol 2019;54:409–18.
[20] D'Orsi CJ, Sickles EA, Mendelson EB, et al.;1; ACR BI-RADS(R) Atlas, Breast Imaging Reporting and Data System, 5th ed. Reston, VA: American College of Radiology; 2013.
[21] Deak P, van Straten M, Shrimpton PC, et al. Validation of a monte carlo tool for patient-specific dose simulations in multi-slice computed tomography. Eur Radiol 2008;18:759–72.
[22] Kyriakou Y, Deak P, Langner O, et al. Concepts for dose determination in flat-detector CT. Phys Med Biol 2008;53:3551–66.
[23] Hupfer M, Kolditz D, Nowak T, et al. Dosimetry concepts for scanner quality assurance and tissue dose assessment in micro-CT. Med Phys 2012;39:658–70.

[24] Westerhof JP, Fischer U, Moritz JD, et al. MR imaging of mammographically detected clustered microcalcifications: is there any value? Radiology 1998;207:675–81.
[25] Bazzocchi M, Zuiani C, Panizza P, et al. Contrast-enhanced breast MRI in patients with suspicious microcalcifications on mammography: results of a multicenter trial. AJR Am J Roentgenol 2006;186:1723–32.
[26] Gilles R, Meunier M, Lucidarme O, et al. Clustered breast microcalcifications: evaluation by dynamic contrast-enhanced subtraction MRI. J Comput Assist Tomogr 1996;20:9–14.
[27] Daskalaki A, Bliznakova K, Pallikarakis N. Evaluation of the effect of silicone breast inserts on X-ray mammography and breast tomosynthesis images: a Monte Carlo simulation study. Phys Med 2016;32:353–61.
[28] Hooley RJ, Scoutt LM, Philpotts LE. Breast ultrasonography: state of the art. Radiology 2013;268:642–59.
[29] Gilbert FJ, Pinker-Domenig K. Diagnosis and Staging of Breast Cancer: When and How to Use Mammography, Tomosynthesis, Ultrasound, Contrast-Enhanced Mammography, and Magnetic Resonance Imaging. In: Hodler J, Kubik-Huch RA, von Schulthess GK, eds. Diseases of the Chest, Breast, Heart and Vessels 2019-2022: Cham (CH): Diagnostic and Interventional Imaging; 2019;155–166.
[30] Sayed A, Layne G, Abraham J, et al. Nonlinear characterization of breast cancer using multi-compression 3D ultrasound elastography in vivo. Ultrasonics 2013;53:979–91.
[31] Goenezen S, Dord JF, Sink Z, et al. Linear and nonlinear elastic modulus imaging: an application to breast cancer diagnosis. IEEE Trans Med Imaging 2012;31:1628–37.
[32] Tabar L, Fagerberg CJ, Gad A, et al. Reduction in mortality from breast cancer after mass screening with mammography. Randomised trial from the Breast Cancer Screening Working Group of the Swedish National Board of Health and Welfare. Lancet 1985;1:829–32.
[33] Swedish Organised Service Screening Evaluation G. Reduction in breast cancer mortality from organized service screening with mammography: 1. Further confirmation with extended data. Cancer Epidemiol Biomarkers Prev 2006;15:45–51.
[34] Yaffe MJ, Mainprize JG. Risk of radiation-induced breast cancer from mammographic screening. Radiology 2011;258:98–105.
[35] Kalender WA, Beister M, Boone JM, et al. High-resolution spiral CT of the breast at very low dose: concept and feasibility considerations. Eur Radiol 2012;22:1–8.
[36] Feig S. Cost-effectiveness of mammography, MRI, and ultrasonography for breast cancer screening. Radiol Clin North Am 2010;48:879–91.
[37] Johnson TR, Himsl I, Hellerhoff K, et al. Dual-energy CT for the evaluation of silicone breast implants. Eur Radiol 2013;23:991–6.
[38] Glazebrook KN, Doerge S, Leng S, et al. Ability of dual-energy CT to detect silicone gel breast implant rupture and nodal silicone spread. AJR Am J Roentgenol 2019;212:933–42.
[39] Tark KC, Jeong HS, Roh TS, et al. Analysis of 30 breast implant rupture cases. Aesthetic Plast Surg 2005;29:460–9. discussion 470-461.
[40] Uhlig J, Fischer U, Surov A, et al. Contrast-enhanced cone-beam breast-CT: analysis of optimal acquisition time for discrimination of breast lesion malignancy. Eur J Radiol 2018;99:9–16.
[41] Arboleda C, Wang Z, Jefimovs K, et al. Towards clinical grating-interferometry mammography. Eur Radiol 2019;30:1419–25.
[42] Li X, Gao H, Chen Z, et al. Diagnosis of breast cancer based on microcalcifications using grating-based phase contrast CT. Eur Radiol 2018;28:3742–50.